

An essential role for Radar (Gdf6a) in inducing dorsal fate in the zebrafish retina

Nathan J. Gosse^a and Herwig Baier^{a,b,1}

Department of Physiology, Programs in ^aDevelopmental Biology, Genetics, and ^bNeuroscience, University of California, 1550 Fourth Street, San Francisco, CA 94158-2722

Edited by Constance L. Cepko, Harvard Medical School, Boston, MA, and approved December 5, 2008 (received for review April 4, 2008)

Retinal ganglion cells form orderly topographic connections with the tectum, establishing a continuous neural representation of visual space. Mapping along the dorsal–ventral axis requires interactions between EphB and ephrin-B cell-surface molecules expressed as countergradients in both retina and tectum. We have discovered that the diffusible TGFβ-related factor Radar (Gdf6a) is necessary and sufficient for activation of dorsal markers, such as Bmp4, Tbx5, Tbx2b, and Ephrin-B2, and suppression of the ventral marker Vax2 in the zebrafish retina. Radar mutant axons innervate only the dorsal half of the tectum, where they form a compressed retinotectal map. Wild-type cells transplanted into the dorsal retina are able to rescue the dorsal identity of nearby mutant cells. Moreover, Radar overexpression “dorsalizes” retinal ganglion cell identity in the ventral retina. We conclude that Radar is near the top of a signaling cascade that establishes dorsal–ventral positional information in the retina and controls the formation of the retinotectal map.

patterning | eye development | ocular coloboma | bone morphogenetic protein | tectum

The dorsal–ventral axis of the retina is specified during embryonic development by signaling mechanisms involving locally secreted factors and spatial gradients of transcription factors (1, 2). These patterning mechanisms eventually provide positional information to retinal ganglion cells (RGCs), which enable their axons to project to the topographically correct target regions in the optic tectum. Axons from dorsally located RGCs project to ventral positions in the tectum, whereas axons of ventral RGCs project to the dorsal half of the tectum (1, 2). This selectivity is achieved by signaling between RGC axons and tectal neurons. Along the dorsal–ventral axes of both the retina and the tectum, expression gradients of EphB and ephrin-B molecules are responsible for translating graded positional information into a smooth retinotectal map (3, 4).

Previous studies have emphasized the importance of bone morphogenetic proteins (Bmps), particularly Bmp4, in dorsalizing retinal tissue through activation of the T-box transcription factor Tbx5. Bmps belong to a family of secreted factors related to TGFβ. Bmp4 has been assigned a central role in dorsal–ventral patterning of the eye, largely based on its expression in the dorsal retina and on results from overexpression in chick, mouse, and *Xenopus* (5–8). Despite compelling gain-of-function effects, however, loss-of-function analysis has yet to support a role for Bmp4 in dorsal–ventral patterning of the eye. Mouse and zebrafish Bmp4 mutants die around gastrulation, or are severely malformed, hampering investigations of their eye phenotypes (9, 10). Heterozygous Bmp4^{+/-} mouse mutants show ocular malformations that appear unrelated to dorsal–ventral patterning (9). A related factor, Bmp2 (Bmp2b in zebrafish) (11) has also been implicated in dorsal patterning of the retina by virtue of its restricted expression in the dorsal retina and its gain-of-function phenotype (12). However, similar to Bmp4, Bmp2 may not be necessary, or even sufficient under physiological conditions, to induce dorsal retinal cell fate. Considering the similarity among Bmp molecules and the promiscuity of their receptors, it is

possible that Bmp4 and/or Bmp2 overexpression adds to a function normally carried out by a different Bmp family member.

In a large-scale chemical mutagenesis screen for disruptions of visual behavior (13), we have recently discovered a zebrafish mutant (initially named *dark half*^{s327}) with small eyes, but otherwise normal external morphology. The mutation is lethal at late-larval or early juvenile stages, with some mutant animals surviving for 21 days postfertilization (dpf). The mutants exhibit a deficit in a subset of behavioral responses to visual stimulation. Injection of axon tracer dyes into the eye of the mutant revealed that only the dorsal half of the tectum was innervated by retinal axons (13). This suggests strongly that the mutation disrupts a genetic locus required for differentiation of dorsal RGCs or for projection of their axons to the ventral tectum.

Here we report that the gene mutated in *dark half*^{s327} encodes the TGFβ-related factor Radar, which belongs to the growth differentiation factor (Gdf) branch of the Bmp family. We show that this secreted molecule is necessary and sufficient to induce dorsal fate in the retina. Loss of this factor prevents specification of RGCs with dorsal identity and thus prevents innervation of the ventral tectum. Conversely, misexpression of Radar is able to override ventralizing signals. Radar activates known dorsal marker expression, notably *bmp4*, *tbx5*, *tbx2b*, and *efnb2*, and represses expression of the ventral fate determinant *vax2*. Overexpression of Bmp4 expands the *tbx5* domain in the zebrafish retina, as it does in chick and mouse, but requires functional Radar for this effect. We arrive at a model in which a gradient of Radar acts in concert with ventral Sonic Hedgehog (Shh) to organize the dorsal–ventral axis of the retina and, thus, one of the axes of the retinotectal map.

Results and Discussion

radar Mutants Have Small Eyes and Retinotectal Mapping Defects.

The external morphology of *radar*^{s327} mutants is inconspicuous, with the exception of their smaller eyes (Fig. 1A). Mutants seem to develop on a normal schedule and inflate their swimbladders after hatching similar to WT. We observed a transient increase in cell death in the embryonic retina of the mutant, which could explain the reduced eye size [supporting information (SI) Fig. S1]. The *radar*^{s327} retina is laminated normally (L. Nevin and H. B., unpublished work) and supports most visual responses (13). The mutants appear darker overall than their WT siblings, which is a result of their failure to contract melanin granules in

Author contributions: N.J.G. and H.B. designed research; N.J.G. performed research; N.J.G. contributed new reagents/analytic tools; N.J.G. and H.B. analyzed data; and N.J.G. and H.B. wrote the paper.

The authors declare no conflict of interest.

This article is a PNAS Direct Submission.

¹To whom correspondence should be addressed. E-mail: herwig.baier@ucsf.edu.

This article contains supporting information online at www.pnas.org/cgi/content/full/0803202106/DCSupplemental.

© 2009 by The National Academy of Sciences of the USA

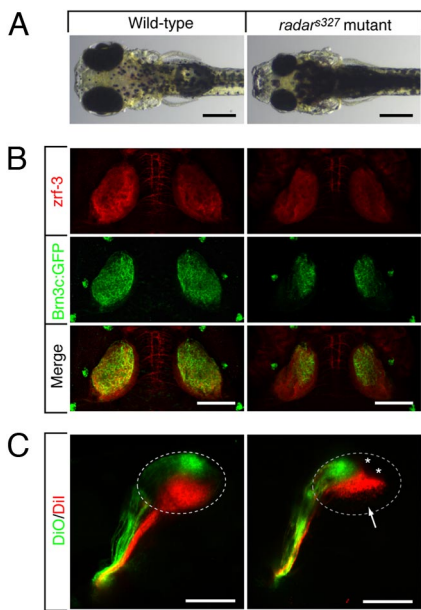


Fig. 1. Morphological and retinotectal phenotypes of *radar*^{s327}. (A) Zebrafish *radar*^{s327} mutants have small eyes and appear dark, because of a VBA defect (see text). Dorsal brightfield views of 7 dpf WT sibling and homozygous *radar*^{s327} mutant larvae. (B) *radar*^{s327} mutants lack ventral innervation of the optic tectum. Dorsal confocal projections of 7 dpf larvae show that innervating RGC axons (expressing *Brn3c:mGFP*) are confined to the dorsal tectum in the mutant. Costaining with a neuropil marker (*zrf-3* antibody) reveals that the size of the tectum is similar in WT and mutant. (C) *radar*^{s327} mutants have a compressed dorsal–ventral retinotectal map. Fixed WT and *radar*^{s327} eyes (7 dpf) were injected with DiO (ventrally) and Dil (dorsally). Lateral confocal projections are shown. Arrow highlights ventral tectal region not innervated by RGCs in *radar*^{s327}; asterisks show positions of skin melanophores. (Scale bars: 300 μ m in A, 100 μ m in B and C.)

their pigment cells in response to light. This neuroendocrine response, termed visual background adaptation (VBA) (14, 15), depends on retinal light perception and transmission of visual signals to the hypothalamus, which in turn control the release of melanin-concentrating hormone from the pituitary. This pathway appears disrupted in the *radar* mutant.

Injection of axon tracer dyes into the eye revealed an abnormal retinotectal projection in *radar*^{s327} mutants (Fig. 1B). In WT larvae, the projection zone of RGC axons, as visualized by the *Brn3c:mGFP* transgene (16), fills the entire dorsal–ventral extent of the tectal neuropil. In *radar*^{s327} mutants, by contrast, retinal axons project to only the dorsal half the tectum. The ventral half of the tectum, although of normal size and apparently fully differentiated, is devoid of retinal afferents. Axon tracing with the lipophilic dyes DiI and DiO injected into the dorsal and ventral retina, respectively, showed that, in the half-innervated *radar*^{s327} tectum, retinotopic order persists (Fig. 1C). Thus, some dorsal–ventral positional information is retained among RGC axons in *radar*^{s327} mutants.

The s327 Mutation Introduces a Stop Codon in *radar* and Abolishes Its Expression in the Dorsal Retina. To identify the genetic lesion responsible for the phenotype, we mapped *s327* to chromosome 16 near marker *z26293* by using a panel of 874 recombinant embryos (17, 18) (Fig. 2A). The *radar* gene, encoding the secreted Bmp-related factor Radar/Gdf6a, represented an excellent candidate for *s327* based on its known expression in the dorsal retina during embryogenesis (19–21) and recent implication as a regulator of retinal marker expression (20, 22, 23). PCR amplification and sequencing of the *radar* cDNA in *radar*^{s327} mutants and WT siblings revealed a single C-to-A trans-

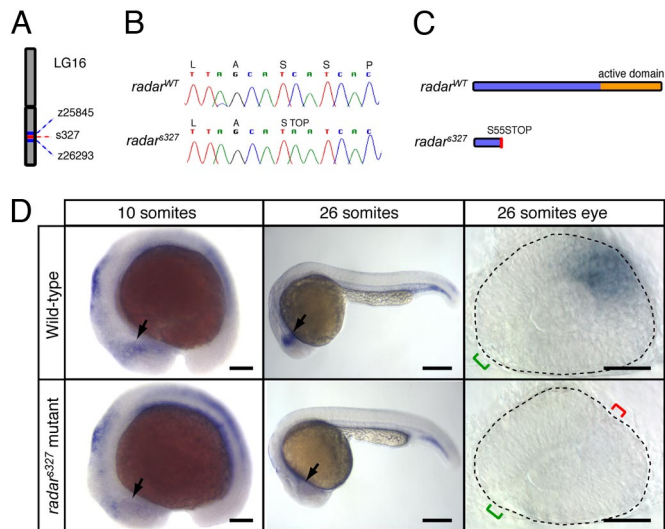


Fig. 2. Positional cloning and expression pattern of *radar*. (A) *s327* maps to chromosome 16 between *z25845* (2.3 cM) and *z26293* (0.7 cM). (B) Sequencing of WT and *s327* cDNA reveals a single C-to-A substitution in position 164 of the *radar* ORF, resulting in a premature stop codon. (C) Predicted translated peptides arising from *radar*^{WT} and *radar*^{s327}. The mutation is predicted to result in a truncated protein, lacking the mature signaling domain. (D) Whole-mount in situ hybridization shows a restricted pattern of *radar* expression in WT embryos. *radar* mRNA is largely absent from the retina of *radar*^{s327} mutants at all stages. In WT, expression is evident in the distal optic vesicle of WT embryos at 10 somites (arrow). At 26 somites, *radar* is expressed dorsally, opposite of the optic fissure (green bracket). Note ectopic fissures (red bracket) in *radar*^{s327} mutants. (Scale bars: 150 μ m for 10 somites, 250 μ m for 26 somites, 50 μ m for dissected 26 somite eyes.)

version, which introduces a stop codon early in the ORF (Fig. 2B). The mutant allele is predicted to encode a truncated pro-protein of 54 aa, which lacks the putative C-terminal mature signaling peptide characteristic of many TGF β proteins (19) (Fig. 2C).

Consistent with a role in dorsal–ventral patterning of the embryonic retina, we found *radar* to be expressed in the distal optic vesicle of WT zebrafish embryos as early as the 10-somite stage, with expression maintained in the dorsal retina beyond the 26-somite stage (Fig. 2D). In *radar*^{s327} mutant embryos, *radar* expression is reduced in the optic vesicle at the 10-somite stage and absent in the retina by the 26-somite stage (Fig. 2D). The early loss of mRNA is likely because of nonsense-mediated decay of the *radar*^{s327} mutant transcript and further suggests a complete loss of zygotic Radar function in *radar*^{s327} mutants. In addition, absence of mRNA may suggest a possible autoregulatory role for *radar*, which is interrupted in the mutant.

Conditional Overexpression of *radar* Rescues Visual Background Adaptation. To confirm that *s327* is a loss-of-function allele of *radar*, we sought to rescue the VBA by reintroducing WT *radar*. Overexpression of *radar* disrupts early gastrulation and axial patterning events (24). We therefore devised a conditional gene expression approach by creating a heatshock-inducible *radar* construct (*hsp70:radar*^{WT}). We confirmed by in situ hybridization that this conditional system was highly effective for misexpression of *radar* in a broadly scattered and variable subset of cells; this mosaicism is likely because of unequal inheritance of the injected plasmid (Fig. S2). To identify the appropriate stage of development, in which *radar* is required for proper eye patterning, we used *hs:dnBMPR* transgenic embryos, in which all Bmp/Gdf signaling is blocked following expression of a dominant-negative receptor (25). Heatshock expression of *dnBMPR*

as early as the 12- to 14-somite stage disrupted dorsal retinal fate (Fig. S3). We reasoned that Radar was likely required in the eye from this stage onwards.

In control clutches from a cross of two heterozygous carriers, VBA-negative (dark) larvae were found near the expected Mendelian frequency (uninjected with heat shock: 26.7%, $n = 105$; injected without heat shock: 20.3%, $n = 69$). Progeny from the same cross injected with 10 ng/ μ L *hsp70:radar*^{WT} and heat-shocked at the 12-somite stage showed a significant reduction in the fraction of VBA-negative larvae (2.2%, $n = 92$). Injection and induced expression of the mutant allele found in *radar*^{s327} mutants (*hsp70:radar*^{s327}) failed to reduce the number of dark larvae (25.4%, $n = 59$). Thus, reintroduction of WT *radar* rescues the VBA.

Radar Overexpression Is Sufficient to Induce Dorsal Retinal Fate. We asked whether *radar* gain of function is sufficient to dorsalize WT cells and to rescue ventral tectum innervation in *radar* mutants. Heterozygous *radar*^{s327} adults carrying *Brn3c:mGFP* were mated and their offspring injected with 25 ng/ μ L *hsp70:radar*^{WT} DNA at the one or two-cell stage. Embryos were then heat-shocked at the 12-somite stage. Injected embryos were raised to 7 dpf and their retinotectal projections investigated. In WT, overexpression of *radar*^{WT} often resulted in embryos with small eyes lacking ventral characteristics (35%; $n = 50$ injected embryos). In these eyes, the optic fissure failed to close, consistent with a loss of ventral retinal identity (26). This is opposite to uninjected *radar*^{s327} mutants, in which an extra fissure could often be detected in the dorsal retina (see Fig. 2D).

In *radar*^{s327} mutants, heatshock-induced expression of *radar*^{WT} restored innervation of the ventral tectum in 60% of the larvae analyzed ($n = 20$; Fig. 3A–C). The stochastic expression pattern of *radar* in these experiments does not allow us to draw strong conclusions about the source of Radar protein necessary for successful rescue of the mutant, but we interpret the failure rate (40%) to cases in which the plasmid was not present in sufficient quantities in the eye (Fig. 3C shows an example of a unilateral retinotectal rescue; see Fig. S2 for evidence of mosaicism). Overexpression of *radar* carrying the point mutation (*hsp70:radar*^{s327}) was not able to rescue the mutant phenotype in $n = 59$ embryos. Heatshock alone ($n = 105$) or injection of *radar*^{WT} alone ($n = 69$) did not change the retinotectal mapping phenotype in either mutant or WT. Together, these experiments demonstrate that Radar is sufficient, when overexpressed, to specify the retinotectal specificity of dorsal RGCs.

Radar Acts on Neighboring Cells in a Position-Dependent Manner. As Gdf6 has previously been shown to be secreted in *Xenopus* (21), we expected that zebrafish Radar could act on neighboring cells in a cell-nonautonomous fashion. We therefore tested whether WT retinal cells could rescue the mutant retinotectal projection by transplanting cells at the blastula stage from WT donors to *radar*^{s327} mutant hosts (the latter labeled with *Brn3c:mGFP*). From a large number of transplantations, 41 chimeras were selected for the presence of small clones of WT cells in the mutant eye. In a majority of them, we observed the rescue of GFP-expressing (i.e., genotypically mutant) axons innervating the ventral tectum (Fig. 3D). This result demonstrated that Radar acts nonautonomously and at physiological concentrations to instruct a dorsal fate.

The positions and clonal sizes of the transplanted cells in the retina were highly variable and difficult to image, making exact quantifications difficult. We nevertheless grouped the chimeras into those with dorsal, ventral, or mixed clone locations. This analysis revealed that the retinotectal projection rescue was limited to cases with WT cells in the dorsal retina, including mixed locations (Fig. S4A and B). Chimeras in which the WT

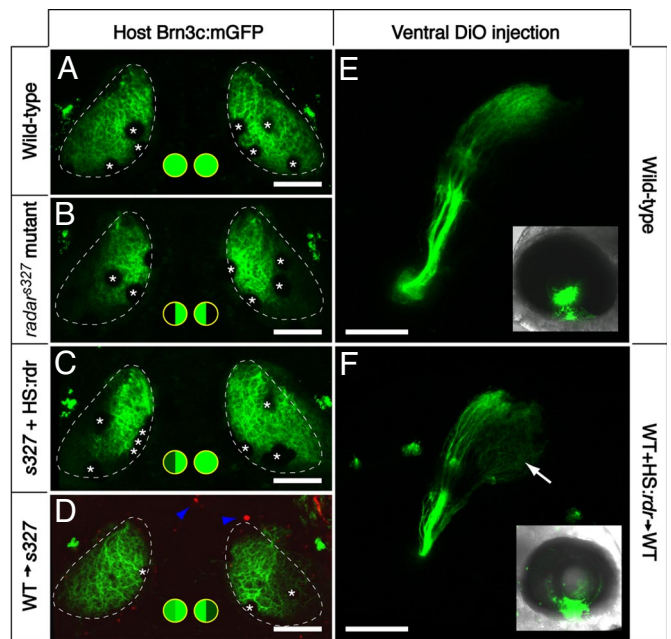


Fig. 3. Cell–cell signaling through Radar is sufficient for ventral tectum innervation. (A–D) Rescue experiment. *Brn3c:mGFP*-labeled retinotectal projections were imaged in vivo at 7 dpf. The tectal neuropil is outlined with a dashed line. Green-filled circles summarize dorsal and ventral tectum innervation results. (A) WT tecta show full innervation. (B) *radar*^{s327} mutants lack ventral innervation. (C) *radar*^{WT} expression from heatshock-promoter rescues the retinotectal phenotype of the mutant. In the case shown, only one side was rescued. PCR-based genotyping confirmed that only the rescued eye contained *hsp70:radar*^{WT}; the other eye had likely not received the injected plasmid because of the mosaicism inherent in transient transgenesis. (D) The *radar* gene acts cell-nonautonomously in the retina. WT cells transplanted into *radar*^{s327} host embryos are sufficient to rescue ventral innervation. Only the host carried the *Brn3c:mGFP* transgene. Donor-derived cells (blue arrowheads) were labeled with rhodamine dextran, and do not contribute to the tectum. (E and F) Gain-of-function experiment. DiO was injected into the ventral retina, and its labeling pattern was imaged from a lateral view. *Insets* show injected eye. In normal WT larvae (E), ventral RGCs project exclusively to the dorsal tectum. In chimeric WT larvae (F) that have received a transplant of WT cells carrying the *hsp70:radar*^{WT} construct, some ventral axons ectopically innervate the ventral tectum (arrow). Asterisks (in A–D) show positions of skin melanophores. (Scale bars, 100 μ m.)

cells were only detectable in the ventral retina were not rescued; they showed a mutant retinotectal phenotype (Fig. S4C and D). Moreover, in rare instances, we encountered chimeras in which the donor cells populated the tissue along the axon tract and in the tectum, but were apparently completely excluded from the retina. The retinotectal projection of these chimeras was also not rescued (Fig. S4E and F). These observations are consistent with a retina-intrinsic and position-dependent role of Radar in patterning the retinotectal map.

We next asked whether Radar misexpression was sufficient to “reprogram” the fate of ventrally located RGCs in WT. For this experiment, we transplanted blastomeres from *hsp70:radar*^{WT} mosaic embryo into a WT host. The resulting chimeras were heat-shocked at the 12-somite stage to induce *radar* expression, sorted for the presence of donor-derived cells in the retina, and allowed to develop. At 7 dpf, DiO was injected at the ventral margin of the retina to label the retinotectal projection. Whereas in all nonheatshocked controls ($n = 10$), DiO-labeled axons projected exclusively to the dorsal tectum (Fig. 3E), in heatshocked chimeras ($n = 3$), axons were seen terminating in the ventral tectum (Fig. 3F). These data suggest that Radar can override ventral-fate determining factors.

on a functional *radar* gene (Fig. 5 B–F; Fig. S5 F and G). The latter finding is significant, because TGF β ligands are known to interact as dimers with their receptor, and several studies have demonstrated that Bmp heterodimers are more potent than homodimers in activating downstream targets (21, 31). The genetic evidence provided here suggests that Radar not only induces *bmp4*, but may also be a necessary component of active Bmp dimers in the dorsal retina (Fig. 5G). Alternatively, Radar may be required for up-regulation of another component without which Bmp4 cannot exert its dorsalizing effect.

A Network of Bmp Factors Patterns Both Embryo and Retina. The central role of Radar shown here is reminiscent of its function during dorsal–ventral axial patterning of the zebrafish embryo (24, 32). Indeed, we found that embryonic and retinal patterning mechanisms share key elements of the underlying signaling pathway. Maternally deposited Radar acts through the type I Bmp receptor Alk8 to induce *bmp2b* (*swirl*) and *bmp4*, which in turn signal through Alk8 to activate ventral factors (10, 24, 32). Another Bmp-encoding gene, *bmp7* (*snailhouse*), is not dependent on induction by Radar (33). We found that Alk8, which is broadly expressed in the retina, appears to serve as a receptor for Radar, as evidenced by reduction of *tbx5* expression in zygotic *lost-a-fin* mutants, in which Alk8 is disrupted (34) (Fig. S5 A and B). Another similarity between retina and early embryo is the independence of *radar* expression from other Bmps; its dorsal–ventral gradient is not detectably altered by manipulations of either *bmp4* or *bmp2b*.

However, the details of how the Bmp ligands interact in the dorsal retina are different from the situation in the pregastrulation embryo. First, Bmp7's role (if any) in the retina is presently unclear. Second, *bmp4* overexpression overrides normal specification, but with differing dependencies on *radar*: ventralization of the early embryo occurs independent of *radar*, while dorsalization of the retina requires *radar* (24). Third, in the retina, Radar is necessary and sufficient for *bmp4* induction. Our findings reveal that there are specific molecular interdependencies of the BMP ligands, which differ between early embryo and retina. The genetic network acting in the retina is summarized in Fig. 5G.

Shh Only Slightly Affects Radar Expression. Although a network of Bmp-related genes specify dorsal retinal fate, hedgehog factors, such as Shh, act in a countergradient to instruct ventral characteristics (26) (see Fig. 5G). Shh, although not expressed in the eye before 28 hpf, is secreted from the midline of the neural tube and promotes ventral expression of *vax* genes (26) and also inhibits dorsal *bmp4* expression (35). We found that *radar* expression is slightly, expanded in the retinas of zebrafish *syu* mutants, which lack Shh (36) (Fig. S5 C and D). Direct interactions between these two signals therefore appear very weak. Residual dorsal–ventral information seen in the retinotectal map of *radar*^{s327} mutants (see Fig. 1C) may thus be conveyed either by genes downstream of Shh (26, 35) or by Radar-independent Bmp signaling (6).

Materials and Methods

Strains and Maintenance. Fish were maintained as previously described (13). Mutant alleles used were *radar/gdf6a*^{s327}, *lost a fin/alk8/lacv1*^{m100}, and *syulshh/shha*^{Δ4}. Transgenic lines used were *Brn3c:mGFP/Tg(pou4f3:gap43-GFP)*^{s356t}, *hs:dnBMPRI/Tg(hsp70:dnBmpr-GFP)*^{w30}, *hs:gal4/Tg(hsp70:Gal4)*^{1.5kca4}, and *hs:bmp2b/Tg(hsp70:bmp2b)*^{fr13}.

Immunohistochemistry. Larvae were raised in with 0.003% (wt/vol) 1-phenyl-2-thiourea (PTU) to inhibit melanin synthesis. Whole-mount TUNEL staining and immunohistochemistry were performed as described elsewhere (37), by using antibodies zrf-3 (Oregon Monoclonal Bank) diluted 1:250, and anti-GFP (Molecular Probes) diluted 1:1000.

Fluorescent Axon Tracing. Dye injections were performed as previously described (13).

Confocal Microscopy. Live larvae were mounted in 1% low melting point agarose in E3 medium and treated with 0.8% norepinephrine to aggregate melanin pigment granules and anesthetized with 0.016% tricaine. Fixed larvae were mounted in 1.6% low melting point agarose in PBS. Confocal imaging was performed with long-working distance lenses (20 \times , NA 0.5; 40 \times , NA 0.8) on a Zeiss Pascal confocal microscope. Images were analyzed and processed with ImageJ and Adobe Photoshop.

Positional Cloning and RFLP Analysis. Linkage mapping was performed as described (13). First strand cDNA was synthesized from 8 dpf homozygous *radar*^{s327} mutants, WT siblings, and homozygous Tüpfel Longfin (WT strain) larval zebrafish. The *radar* ORF was amplified by PCR using specific primer sequences (forward 5'-ATGGATGCTTGAGAGCAGTC-3' and reverse 5'-CTACCTGCAGCCACTGTC-3'). The s327 mutation destroys an SfaNI site, allowing identification of carriers by restriction fragment length polymorphism (RFLP) analysis. Amplification from genomic DNA by PCR with the forward primer and the RFLP reverse primer (5'-TTGAGAGCG-GAAAAAGCTC-3'), followed by digestion with SfaNI resulted in products of 170 and 110 bp in WT and a single band of 280 bp from *radar*^{s327} mutants.

In situ Hybridization. Dig-labeled riboprobes for full-length *radar*, *tbx2b*, *tbx5*, *bmp2b* and *vax2* were transcribed in vitro. *radar*^{s327} mutants and WT siblings were stained as a clutch, with expected mutant frequencies of 25%. *laf* and *syu* mutants were sorted before staining, then treated with identical conditions. Whole-mount in situ hybridizations were carried out as previously described (38) and stored in 87% glycerol. Eyes were dissected using tungsten needles and mounted in a similar orientation. For *bmp4*-, *tbx5*-, and *vax2*-stained embryos lacking staining in the retina, eyes were dissected from animals that had comparable staining in other tissues. All images were collected with a Leica dissection microscope or a Zeiss compound microscope equipped with a Spot CCD camera (Diagnostic Instruments) or AxioCam MRC (Zeiss), and prepared by using Adobe Photoshop.

radar^{s327} mutant and WT sibling embryos were genotyped by RFLP analysis (see above), with DNA isolated before imaging by clipping the trunk, or following imaging using the entire embryo. DNA was isolated by methanol dehydration, tissue maceration, and overnight incubation in 1.7 mg/ μ L proteinase-K (Roche) in 10 mM Tris, pH 8.0.

Injection and Heatshock Induction. The *radar* ORF was amplified with modified forward and reverse cloning primers (see above) containing Sall restriction sites, and subcloned downstream of the *hsp70* promoter in a construct flanked by Tol2 transposase recognition sites (39). For all rescue experiments, 10 ng/ μ L DNA was coinjected with 25 ng/ μ L Tol2 transposase mRNA, and 25 ng/ μ L GFP mRNA generated with the mMessage mMachin kit (Ambion) at the 1–2 cell stage. Poorly injected (identified by a lack of strong GFP fluorescence) and malformed embryos were excluded from the experiment before heatshock. Heatshock induction was carried out as described (25).

The *bmp4* ORF was amplified by PCR and Xi cloned (Gene Technology Systems) into a vector containing 14 repeats of the upstream activating sequence (UAS), and flanked by Tol2 sequences (39). 10 ng/ μ L DNA was injected into an in-cross of carriers of the s327 mutation and the *hsp70:gal4* transgene. Heatshock induction was carried out at 12 somites to allow sufficient time for Gal4-mediated transactivation. Similar injection controls were done, and only animals with increased trunk and tail thickness indicative of BMP overexpression were kept for staining. Heatshock-induced overexpression of *bmp2b* was similarly achieved by using transgenic embryos (40).

Transplantation Experiments. Donor embryos were injected with a solution of 1–5% tetramethyl-rhodamine dextran amine (Molecular Probes). Blastula-stage transplants were performed as described (38). Chimeras were sorted at 30–36 hours postfertilization (hpf) for the presence of rhodamine-positive cells in the neural retina and treated with PTU. For overexpressing chimera experiments, donors were also coinjected with 25 ng/ μ L *hsp70:radar*^{WT}, 25 ng/ μ L Tol2 transposase mRNA, and 25 ng/ μ L GFP mRNA. Following heatshock at 12 somites, chimeras were sorted and treated as above.

Morpholino Knockdown. Morpholino target sequences for *bmp4* (40) and *bmp2b* knockdown (41) were published elsewhere.

ACKNOWLEDGMENTS. We thank D. Stainier (University of California, San Francisco), A. Picker (Max-Planck-Institut of Molecular Cell Biology and Genetics), M. Mullins (University of Pennsylvania), and the Zebrafish Inter-

national Resource Center for reagents and fish strains, and J. Pinkston-Gosse and members of the Baier lab for review of the manuscript. This work

was funded by the March of Dimes Foundation and the National Institutes of Health.

1. Harada T, Harada C, Parada LF (2007) Molecular regulation of visual system development: More than meets the eye. *Gene Dev* 21:367–378.
2. McLaughlin T, Hindges R, O'Leary DD (2003) Regulation of axial patterning of the retina and its topographic mapping in the brain. *Curr Opin Neurobiol* 13:57–69.
3. Hindges R, McLaughlin T, Genoud N, Henkemeyer M, O'Leary DD (2002) EphB forward signaling controls directional branch extension and arborization required for dorsoventral retinotopic mapping. *Neuron* 35:475–487.
4. Mann F, Ray S, Harris W, Holt C (2002) Topographic mapping in dorsoventral axis of the *Xenopus* retinotectal system depends on signaling through ephrin-B ligands. *Neuron* 35:461–473.
5. Koshiba-Takeuchi K, et al. (2000) Tbx5 and the retinotectum projection. *Science* 287:134–137.
6. Behesti H, Holt JK, Sowden JC (2006) The level of BMP4 signaling is critical for the regulation of distinct T-box gene expression domains and growth along the dorsoventral axis of the optic cup. *BMC Dev Biol* 6:62.
7. Sasagawa S, Takabatake T, Takabatake Y, Muramatsu T, Takeshima K (2002) Axes establishment during eye morphogenesis in *Xenopus* by coordinate and antagonistic actions of BMP4, Shh, and RA. *Genesis* 33:86–96.
8. Trousse F, Esteve P, Bovolenta P (2001) Bmp4 mediates apoptotic cell death in the developing chick eye. *J Neurosci* 21:1292–1301.
9. Chang B, et al. (2001) Haploinsufficient Bmp4 ocular phenotypes include anterior segment dysgenesis with elevated intraocular pressure. *BMC Genet* 2:18.
10. Stickney HL, Imai Y, Draper B, Moens C, Talbot WS (2007) Zebrafish *bmp4* functions during late gastrulation to specify ventroposterior cell fates. *Dev Biol* 310:71–84.
11. Kishimoto Y, Lee KH, Zon L, Hammerschmidt M, Schulte-Merker S (1997) The molecular nature of zebrafish swirl: BMP2 function is essential during early dorsoventral patterning. *Development* 124:4457–4466.
12. Sakuta H, et al. (2006) Role of bone morphogenetic protein 2 in retinal patterning and retinotectal projection. *J Neurosci* 26:10868–10878.
13. Muto A, et al. (2005) Forward genetic analysis of visual behavior in zebrafish. *PLoS Genet* 1:e66.
14. Neuhauss SC, et al. (1999) Genetic disorders of vision revealed by a behavioral screen of 400 essential loci in zebrafish. *J Neurosci* 19:8603–8615.
15. Kay JN, Finger-Baier KC, Roeser T, Staub W, Baier H (2001) Retinal ganglion cell genesis requires *lakritz*, a Zebrafish atonal Homolog. *Neuron* 30:725–736.
16. Xiao T, Roeser T, Staub W, Baier H (2005) A GFP-based genetic screen reveals mutations that disrupt the architecture of the zebrafish retinotectal projection. *Development* 132:2955–2967.
17. Shimoda N, et al. (1999) Zebrafish genetic map with 2000 microsatellite markers. *Genomics* 58:219–232.
18. Knapik EW, et al. (1998) A microsatellite genetic linkage map for zebrafish (*Danio rerio*). *Nat Genet* 18:338–343.
19. Rissi M, Wittbrodt J, Delot E, Naegeli M, Rosa FM (1995) Zebrafish Radar: A new member of the TGF-beta superfamily defines dorsal regions of the neural plate and the embryonic retina. *Mech Dev* 49:223–234.
20. Asai-Coakwell M, et al. (2007) GDF6, a novel locus for a spectrum of ocular developmental anomalies. *Am J Hum Genet* 80:306–315.
21. Chang C, Hemmati-Brivanlou A (1999) *Xenopus* GDF6, a new antagonist of noggin and a partner of BMPs. *Development* 126:3347–3357.
22. Hanel ML, Hensley C (2006) Eye and neural defects associated with loss of GDF6. *BMC Dev Biol* 6:43.
23. French CR, et al. (2007) Pbx homeodomain proteins pattern both the zebrafish retina and tectum. *BMC Dev Biol* 7:85.
24. Sidi S, Goutel C, Peyrieras N, Rosa FM (2003) Maternal induction of ventral fate by zebrafish radar. *Proc Natl Acad Sci USA* 100(6):3315–3320.
25. Pyati UJ, Webb AE, Kimelman D (2005) Transgenic zebrafish reveal stage-specific roles for Bmp signaling in ventral and posterior mesoderm development. *Development* 132:2333–2343.
26. Takeuchi M, Clarke JD, Wilson SW (2003) Hedgehog signalling maintains the optic stalk-retinal interface through the regulation of Vax gene activity. *Development* 130:955–968.
27. Barbieri AM, et al. (1999) A homeobox gene, *vax2*, controls the patterning of the eye dorsoventral axis. *Proc Natl Acad Sci USA* 96(19):10729–10734.
28. Mui SH, Hindges R, O'Leary DD, Lemke G, Bertuzzi S (2002) The homeodomain protein Vax2 patterns the dorsoventral and nasotemporal axes of the eye. *Development* 129:797–804.
29. Schulte D, Furukawa T, Peters MA, Kozak CA, Cepko CL (1999) Misexpression of the *Emx*-related homeobox genes *cVax* and *mVax2* ventralizes the retina and perturbs the retinotectal map. *Neuron* 24:541–553.
30. Gross JM, Dowling JE (2005) Tbx2b is essential for neuronal differentiation along the dorsal/ventral axis of the zebrafish retina. *Proc Natl Acad Sci USA* 102:4371–4376.
31. Butler SJ, Dodd J (2003) A role for BMP heterodimers in roof plate-mediated repulsion of commissural axons. *Neuron* 38:389–401.
32. Goutel C, Kishimoto Y, Schulte-Merker S, Rosa F (2000) The ventralizing activity of Radar, a maternally expressed bone morphogenetic protein, reveals complex bone morphogenetic protein interactions controlling dorso-ventral patterning in zebrafish. *Mech Dev* 99:15–27.
33. Wilm TP, Solnica-Krezel L (2003) Radar breaks the fog: Insights into dorsoventral patterning in zebrafish. *Proc Natl Acad Sci USA* 100:4363–4365.
34. Mintzer KA, et al. (2001) Lost-a-fin encodes a type I BMP receptor, Alk8, acting maternally and zygotically in dorsoventral pattern formation. *Development* 128:859–869.
35. Zhang XM, Yang XJ (2001) Temporal and spatial effects of Sonic hedgehog signaling in chick eye morphogenesis. *Dev Biol* 233:271–290.
36. Schauerte HE, et al. (1998) Sonic hedgehog is not required for the induction of medial floor plate cells in the zebrafish. *Development* 125:2983–2993.
37. Wehman AM, Staub W, Meyers JR, Raymond PA, Baier H (2005) Genetic dissection of the zebrafish retinal stem-cell compartment. *Dev Biol* 281:53–65.
38. Kay JN, Link BA, Baier H (2005) Staggered cell-intrinsic timing of *ath5* expression underlies the wave of ganglion cell neurogenesis in the zebrafish retina. *Development* 132:2573–2585.
39. Scott EK, et al. (2007) Targeting neural circuitry in zebrafish using GAL4 enhancer trapping. *Nat Methods* 4:323–326.
40. Shin D, et al. (2007) Bmp and Fgf signaling are essential for liver specification in zebrafish. *Development* 134:2041–2050.
41. Imai Y, Talbot WS (2001) Morpholino phenocopies of the *bmp2b/swirl* and *bmp7/snailhouse* mutations. *Genesis* 30:160–163.